Imaging Features of Pediatric Sarcoidosis

Gozde Ozer, MD • H. Nursun Ozcan, MD • Rahsan Gocmen, MD • Diclehan Orhan, MD • Berna Oguz, MD • Mithat Haliloglu, MD

Author affiliations, funding, and conflicts of interest are listed at the end of this article.

Sarcoidosis is a granulomatous inflammatory disease of uncertain cause. It occurs most commonly in young and middle-aged adults and less frequently in children; therefore, few data on pediatric sarcoidosis exist in the literature. The diagnosis and management of sarcoidosis remain challenging because of diverse and often nonspecific clinical and imaging findings. In addition, the clinical picture varies widely by age. Prepubertal and adolescent patients often present with adult-like pulmonary disease; however, early-onset sarcoidosis is typically characterized by the triad of arthritis, uveitis, and skin rash. Sarcoidosis is mostly a diagnosis of exclusion made by demonstrating noncaseating granulomas at histopathologic examination in patients with compatible clinical and radiologic findings. Although sarcoidosis often affects the lungs and thoracic lymph nodes, it can involve almost any organ in the body. The most common radiologic manifestation is pulmonary involvement, characterized by mediastinal and bilateral symmetric hilar lymphadenopathies with perilymphatic micronodules. Abdominal involvement is also common in children and often manifests as hepatomegaly, splenomegaly, and abdominal lymph node enlargement. Although neurosarcoidosis and cardiac sarcoidosis are rare, imaging is essential to the diagnosis of central nervous system and cardiac involvement because of the risky biopsy procedure and its low diagnostic yield due to focal involvement. Being familiar with the spectrum of imaging findings of sarcoidosis may aid in appropriate diagnosis and management.

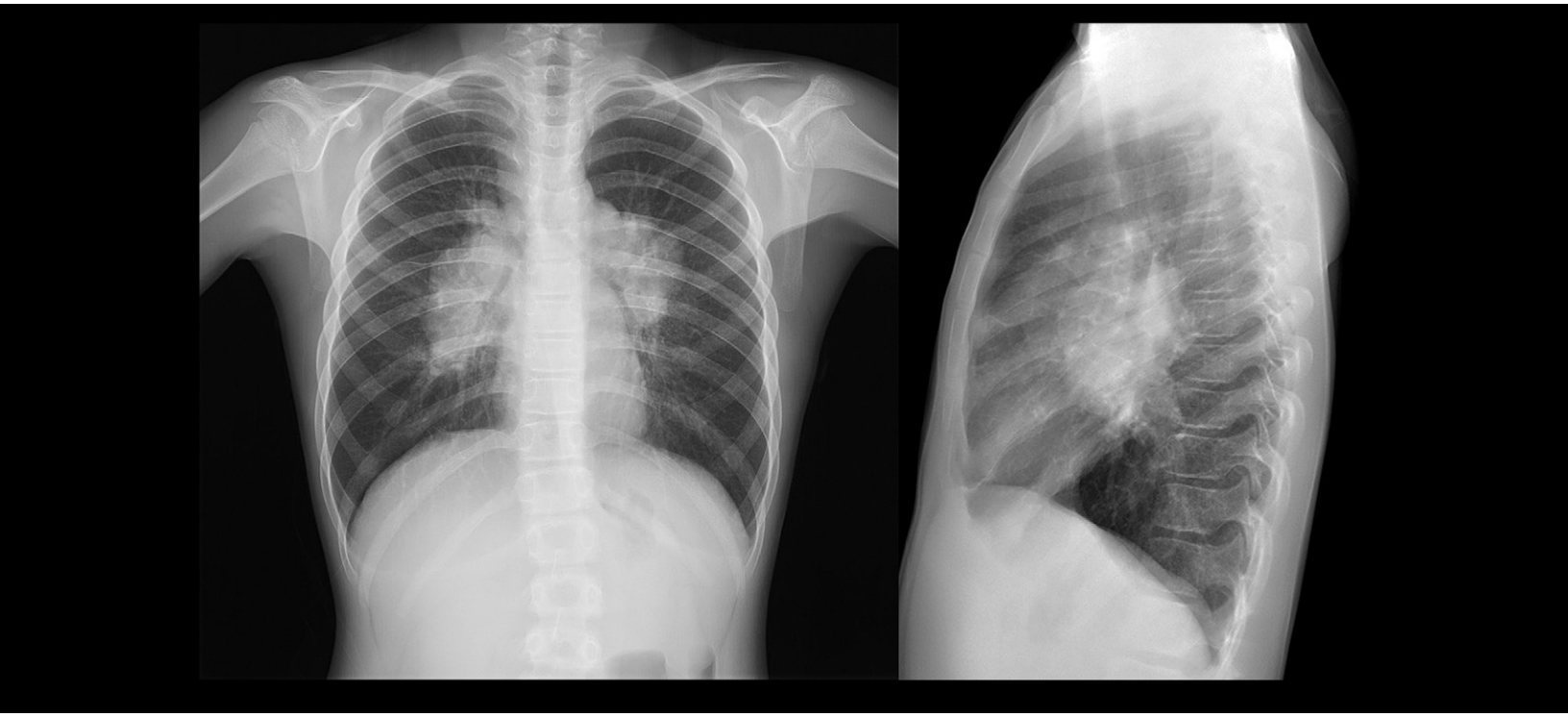

Introduction

Sarcoidosis is a multisystem granulomatous disease of uncertain cause characterized by the development of noncaseating granulomas. It occurs most commonly in young and middle-aged adults, and so its clinical and radiologic features have been extensively investigated in adult patients. However, it occurs 10 times less frequently in children (1,2), and although research dates back 7 decades since its first review (3), there are still few data on pediatric sarcoidosis in the literature, to our knowledge.

Although it is difficult to determine the true incidence of childhood sarcoidosis because of the rarity of the disease and the paucity of published data, it has been reported as 0.6–1.02 cases per 100 000 children (1). The incidence does not substantially differ according to sex but it is more common in Black children (4–6). Retrospective case series (4–7) show that

Supplemental Material

Test Your Knowledge questions are available in the supplemental material.

RadioGraphics 2024; 44(1):e230098
https://doi.org/10.1148/rg.230098

Content Codes: CH, CT, MR, PD

Abbreviations: CNS = central nervous system, CSF = cerebrospinal fluid, FDG = fluorodeoxyglucose, GI = gastrointestinal

TEACHING POINTS

- Hilar and mediastinal lymphadenopathies with interstitial pulmonary involvement are the most common radiologic manifestations of sarcoidosis in both children and adults. However, multiorgan involvement is more common in children, and three or more organs are involved in more than 70% of cases.
- The characteristic parenchymal pattern in pulmonary involvement is well-defined perilymphatic micronodules formed by aggregation of the noncaseating granulomas, which is the histologic hallmark of sarcoidosis. In both children and adults, perifissural, peribronchovascular, and subpleural micronodules with a predominance in the middle and upper zones are the most common parenchymal abnormalities.
- Hepatic and splenic sarcoidosis usually manifest as hepatosplenomegaly but may also manifest as multiple granulomatous nodules in the parenchyma.
- The most common imaging findings in pediatric patients with neurosarcoidosis are leptomeningeal and cranial nerve enhancement, hypothalamic-pituitary involvement, and parenchymal disease manifesting as multiple subcortical and periventricular white matter lesions.
- Although arthritis is the most common form of musculoskeletal sarcoidosis in children, radiologically evident involvement is relatively rare. Chronic nonerosive polyarthritis affecting the appendicular skeleton, particularly the knees, ankles, wrists, and proximal interphalangeal joints, is a common feature of sarcoid joint disease.

reported patients are predominantly of African-Caribbean, sub-Saharan African, and European origin. Sarcoidosis can affect children of all ages; however, approximately two-thirds of patients are older than 10 years at diagnosis (4–6). The clinical spectrum and prognosis vary widely by age and ethnicity (7,8). Most diagnoses in the pediatric age group occur during preadolescence or adolescence, and these cases resemble adult-like disease characterized by interstitial pulmonary involvement and hilar lymphadenopathies. Early-onset sarcoidosis and its counterpart, Blau syndrome, can be diagnosed by the presence of the triad of arthritis, uveitis, and skin rash in children younger than 5 years of age (9). Blau syndrome refers to the hereditary form of early-onset sarcoidosis and results from one of many possible single variants in the *NOD2* gene (10).

Despite extensive research, the pathogenesis of sarcoidosis remains elusive. It is generally accepted that the dysregulated immune system, characterized by an exaggerated cellular immune response to environmental antigens, leads to a chronic inflammatory process in genetically susceptible individuals. Familial clustering and racial differences in the incidence of sarcoidosis support the argument that the disease may be genetic. Human leukocyte antigen types have been shown to be associated with the development, clinical course, and prognosis of the disease. Genetic predisposition is an important risk factor; having a family member with sarcoidosis is associated with a two- to fourfold increase in risk (11). In addition to genetic susceptibility, exposure to inorganic particles has been reported to increase the risk of sarcoidosis in pediatric patients (12).

Sarcoid granulomas can affect any organ of the body, and the wide variation in the rates of organ involvement in the literature is probably due to the lack of a precise definition of involvement. Hilar and mediastinal lymphadenopathies with interstitial pulmonary involvement are the most common radiologic manifestations of sarcoidosis in both children and adults. However, multiorgan involvement is more common in children, and three or more organs are involved in more than 70% of cases (4,5,7). The imaging manifestations vary widely depending on which systems are involved (Table). Because of the diverse and often nonspecific clinical and imaging findings, sarcoidosis is sometimes referred to as "the great masquerader." The diagnosis and management of pediatric sarcoidosis remain challenging because of the lack of consensus on the diagnostic criteria and the standardized diagnostic approach and the unpredictability of the clinical course. Imaging can contribute to the management of the disease by allowing assessment of the extent and activity of sarcoidosis. However, there are few data on imaging manifestations of the disease in the literature, most of which are limited to anecdotal case reports. In this article, we review the imaging features of pulmonary and extrapulmonary pediatric sarcoidosis.

Histopathology and Pathogenesis

The presence of noncaseating granulomas, which are thought to result from a dysregulated immune response to environmental antigens, is the histologic hallmark of sarcoidosis (Fig 1). A sarcoid granuloma is a circumscribed area of granulomatous inflammation containing epithelioid cells, giant cells, and CD4+ T cells in its center and CD8+ T cells, fibroblasts, and B cells at the periphery (13). Some cytoplasmic inclusions, such as asteroid bodies, Schaumann bodies, and Hamazaki-Wesenberg bodies, can be identified within granulomas and can suggest the diagnosis of sarcoidosis; however, they are not pathognomonic (13).

Nonnecrotizing granuloma formation is possibly an immune mechanism to isolate the nondegradable antigen (14). After exposure, interaction between antigen-presenting cells and CD4+ T cells triggers an immune response by means of molecules of the major histocompatibility complex class II. Activated CD4+ cells transform into T helper cells and secrete predominantly interleukin-2 and interferon-γ, which increases macrophage tumor necrosis factor-α production, causing an exaggerated local cellular immune response (14). Cytokines promote granuloma formation, which is a core of epithelioid cells surrounded by lymphocytes, primarily CD4+ T cells, some CD8+ T cells, and B cells. Sarcoid granulomas often spontaneously regress because of various immunologic interactions; however, chronic cytokine stimulation can also result in fibrosis in granulomas (14).

Clinical Features

Children with sarcoidosis present with a broad spectrum of clinical manifestations, ranging from the subclinical form to severe multiorgan disease. Symptoms depend on the intensity of inflammation and which organs are affected, and many symptoms, such as hypercalcemia and fatigue, are caused not by granulomas in a particular location but by the release of mediators (14).

Common Radiologic Features of Pediatric Sarcoidosis in Different Organ Systems

Common Involvement Sites	Imaging Findings
Chest	
Hilar and mediastinal lymph nodes	Bilateral hilar and mediastinal enlarged lymph nodes at chest radiography and CT
Lungs	Perifissural, peribronchovascular, and subpleural micronodules at CT
Abdomen: spleen and liver	Hepatosplenomegaly and nodular involvement; sarcoid nodules are hypoechoic at US, hypoattenuating at CT, and hypointense at T1- and T2-weighted MRI
Central nervous system	
Leptomeninges and cranial nerves	Diffuse or nodular thickening and contrast enhancement of the leptomeninges, with a basilar predilection and enlargement and enhancement of the affected cranial nerve at postcontrast T1-weighted MRI
Hypothalamus and pituitary gland	Thickening and enhancement of the pituitary stalk at postcontrast T1-weighted MRI
Head and neck	
Orbital	Diffuse enlargement and enhancement of the lacrimal gland at CT and MRI
Parotid gland	Enlargement and hypoechogenicity at US, increased signal intensity at T2-weighted MRI, and homogeneous enhancement at postcontrast T1-weighted MRI
Musculoskeletal system	
Joints	Chronic nonerosive arthritis, with nonspecific imaging findings, including synovitis and/or tenosynovitis
Bones	Lacelike lytic lesions in small bones of the hands and feet at radiography

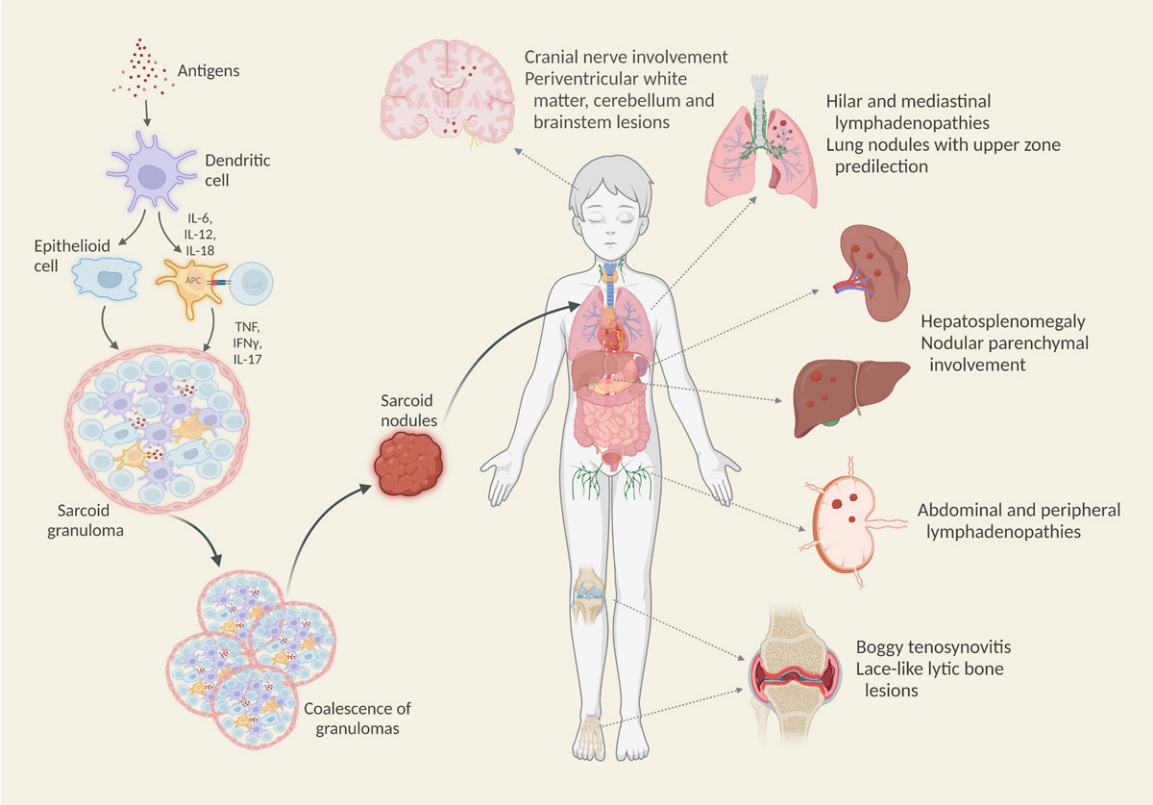

Figure 1. Simplified illustration of the granuloma formation cascade and common involvement patterns of pediatric sarcoidosis by organ system. *IFN* = interferon, *IL* = interleukin, *TNF* = tumor necrosis factor. (Created with BioRender.com.)

There are notable differences in presentation between adults and children, and constitutional symptoms and multiorgan involvement are much more common in the pediatric age group (15,16). In addition, the presentation and clinical findings of the disease in children vary according to age. Whereas younger patients usually present with systemic

symptoms, skin involvement, and hepatosplenomegaly, thoracic disease–related symptoms are more common in older patients (7). The most common symptoms in children are fatigue, fever, and weight loss (4–6). In addition to nonspecific symptoms, respiratory symptoms such as chest pain, dyspnea, and dry cough are common; however, children with lung and mediastinal involvement may still be asymptomatic (4). Other common manifestations in children include peripheral lymphadenopathy, uveitis, erythematous skin rash, hepatosplenomegaly, and arthritis (7,17).

Currently, the main treatment of childhood sarcoidosis is corticosteroid medication. Immunosuppressive agents, particularly methotrexate, are another option for patients with steroid-resistant disease and those experiencing the adverse effects of long-term steroid use (7). The clinical course of pediatric sarcoidosis ranges from spontaneous regression to irreversible organ failure. Many unfavorable prognostic factors have been described in adults with sarcoidosis, such as advanced age at onset, Black race, and radiologic findings that include pulmonary fibrosis and isolated lung involvement (18). However, some of these factors may not be suitable for predicting the prognosis of patients with pediatric sarcoidosis, although multiorgan involvement has been associated with relapse in children, as is seen in adults (4,16). Although early-onset sarcoidosis was believed to be associated with an adverse prognosis (19), Nathan et al (4) reported that younger age at diagnosis was not related to an adverse prognosis. The prognosis of childhood sarcoidosis in White persons has been reported to be favorable, and most patients recover (20). On the other hand, Chauveau et al (16) noted persistent disease into adulthood in almost one-half of patients, most of whom were of African and Caribbean origin.

Diagnosis

Pediatric sarcoidosis is often a diagnosis of exclusion, because there is no definitive and reliable diagnostic test. Rigorous investigations are required in patients with suspected sarcoidosis, including clinical history, physical examination, laboratory tests, and imaging. Laboratory test results may reveal increased acute phase reactants, anemia, and hypercalcemia (17,21). Although liver involvement is relatively common in children, more than one-half of patients with hepatomegaly had normal serum aminotransferase levels (5). Serum angiotensin-converting enzyme is also a well-known serum biomarker in sarcoidosis. However, it has limited diagnostic value because of its low sensitivity and specificity (22). Levels of lysozyme, neopterin, serum interleukin-2 receptor, chitotriosidase, and B-cell activating factor may be useful for predicting treatment response and disease activity (22). The definitive diagnosis of sarcoidosis is generally based on three criteria: compatible clinical and radiologic findings; observation of a noncaseating granuloma at histopathologic examination of the affected tissue; and exclusion of other causes of granuloma, such as mycobacterial or fungal infections (23).

Chest radiography is a routine part of the diagnostic workup for sarcoidosis and is often used to investigate the spread of thoracic disease and to monitor treatment response. Although CT is known to be superior in monitoring thoracic disease, chest radiography is still the preferred first step, especially during follow-up, because of the high radiation exposure at CT. Owing to existing and emerging techniques, MRI is increasingly used for chest imaging in children. MRI can depict not only mediastinal and hilar abnormalities but also parenchymal disease without using ionizing radiation, so it should be considered as an alternative to CT and radiography in the diagnosis and follow-up of sarcoidosis (24). Because multiorgan involvement is more prevalent in children, US, CT, and MRI are helpful in investigating systemic involvement. Gallium 67 (^{67}Ga)–citrate scintigraphy and fluorine 18 (^{18}F) fluorodeoxyglucose (FDG) PET/CT may also be useful in detecting clinically silent disease and assessing the response to treatment (25).

Pulmonary Sarcoidosis

The lungs and hilar lymph nodes are commonly affected organs in children with sarcoidosis, even in patients without respiratory symptoms (26). Bilateral hilar lymphadenopathy can be discovered as an incidental finding during a routine medical examination (27). At the time of diagnosis, 45%–89% of children with sarcoidosis have positive findings on chest radiographs (1,6,26). Although chest radiography is often the first step, CT can depict parenchymal abnormalities and mediastinal lymphadenopathies with higher sensitivity (28). Therefore, CT is routinely used in children with suspected sarcoidosis. It also is commonly used to evaluate clinical or radiologic findings that are not consistent with sarcoidosis, to visualize subtle parenchymal findings, or to identify complications.

In 1961, Scadding (29) developed a staging system for sarcoidosis based on chest radiographic findings. The Scadding staging system is still widely used in adults because of its prognostic value, although no such association has been found in children. Possible explanations are the small number of patients studied and the lack of stage 4 disease at the time of diagnosis (4). Despite its questionable value for prediction of the clinical course, the staging system is routinely used in children. The Scadding system defines five stages of sarcoidosis: stage 0, normal chest radiography; stage 1, only thoracic lymphadenopathy; stage 2, thoracic lymphadenopathy with parenchymal lung disease; stage 3, only parenchymal lung disease; stage 4, pulmonary fibrosis. At presentation, 10%–50% of children with sarcoidosis have normal chest radiographs (5,26). Stage 1 disease is the most common imaging finding in children with thoracic disease (Fig 2); stage 2 disease and stage 3 disease have been reported with varying frequency in different case series (30). Pulmonary fibrosis consistent with stage 4 disease was not noted in any pediatric patients at diagnosis (5,6,16,26). Radiologic findings were reported to regress in most patients during long-term follow-up, and pulmonary findings progressed to stage 4 in only a small number of patients (16,31).

Stage 1 disease with bilateral symmetric hilar and right paratracheal lymphadenopathies are common in patients presenting with thoracic disease. However, because sarcoidosis is rare in children and is usually a diagnosis of exclusion,

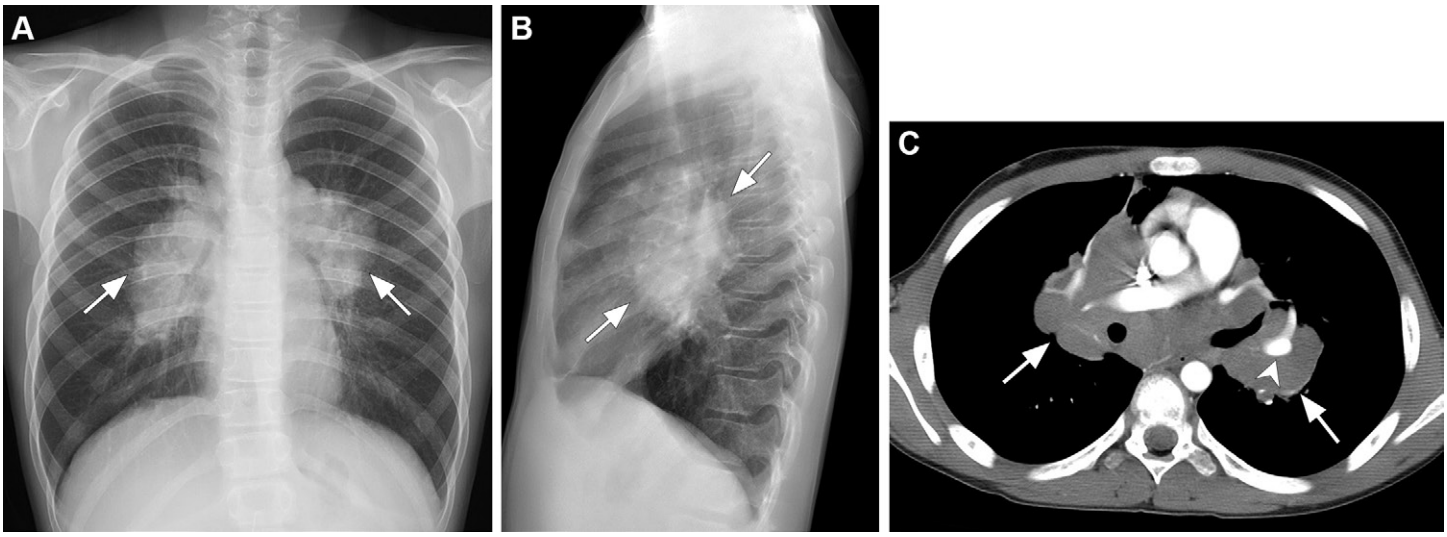

Figure 2. Thoracic sarcoidosis in a 12-year-old boy. **(A, B)** Posteroanterior **(A)** and lateral **(B)** radiographs show bilateral hilar and mediastinal lymphadenopathies (arrows) without parenchymal disease (stage 1). **(C)** Axial CT image (mediastinal window) confirms mediastinal and hilar lymphadenopathies (arrows), without vascular compression (arrowhead).

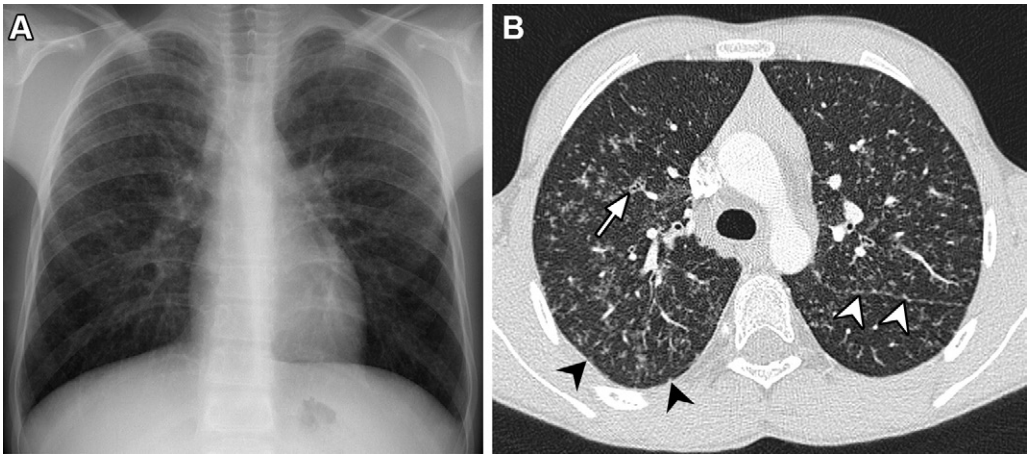

Figure 3. Pulmonary sarcoidosis in a 15-year-old adolescent boy. **(A)** Chest radiograph shows bilateral upper lobe–predominant micronodular opacities and left hilar lymphadenopathy consistent with stage 2 disease. **(B)** Axial chest CT image (lung window) shows micronodules with perilymphatic distribution through fissures (white arrowheads), interlobular septa, bronchovascular bundles (arrow), and subpleural nodules (black arrowheads).

other causes of lymphadenopathy for the differential diagnosis should be ruled out first. Intrathoracic lymph node enlargement can occur in a variety of pediatric diseases, including infections (eg, tuberculosis, bacterial or viral pneumonia, and fungal infection), lymphoma, metastasis, and Castleman disease (32). Lymphadenopathies in sarcoidosis are usually nonnecrotic and noncompressive, unlike those seen in tuberculosis, in which the lymph nodes typically have central necrosis and peripheral rim enhancement (33,34). In addition, calcifications within lymph nodes indicate latent tuberculosis. Nodal calcifications may occur in adult pulmonary sarcoidosis and are related to the duration of the disease but have never been reported in children (35). Another principal consideration in the differential diagnosis is lymphoma, which is the most common cause of a mediastinal mass in children. Lymphoma usually manifests as a mass in the prevascular mediastinum; however, it may also manifest with hilar and mediastinal lymphadenopathies, as seen in sarcoidosis (32). Because peripheral lymphadenopathies, hepatosplenomegaly, and constitutional symptoms are common in both lymphoma and sarcoidosis, histopathologic examination is essential for diagnosis. In addition, atypical patterns such as mediastinal lymphadenopathies without enlargement of the hilar lymph nodes and unilateral hilar lymphadenopathies are rare in sarcoidosis and should prompt investigation for alternative diagnoses (35).

The characteristic parenchymal pattern in pulmonary involvement is well-defined perilymphatic micronodules formed by aggregation of the noncaseating granulomas, which is the histologic hallmark of sarcoidosis (Fig 3) (36). In both children and adults, perifissural, peribronchovascular, and subpleural micronodules with a predominance in the middle and upper zones are the most common parenchymal abnormalities (37,38). Although these parenchymal findings on CT images are highly characteristic of sarcoidosis, they are not pathognomonic and can be observed in various pulmonary parenchymal diseases. However, pulmonary Langerhans cell histiocytosis and miliary tuberculosis should be considered in the differential diagnosis. Pulmonary Langerhans cell histiocytosis, also characterized by multiple bilateral symmetric nodules with a predilection for the upper and middle zones, can be distinguished from sarcoidosis by the centrilobular distribution

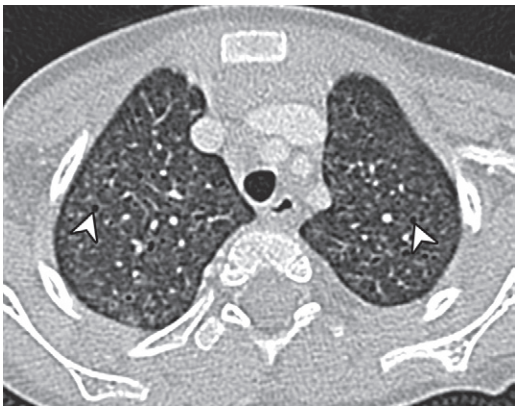

Figure 4. Langerhans cell histiocytosis in a 2-year-old boy. Axial CT image (lung window) shows multiple ill-defined centrilobular nodules and thin-walled small cysts (arrowheads) in bilateral upper lung lobes.

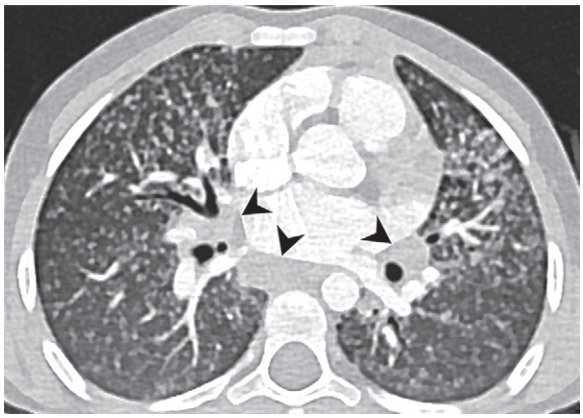

Figure 5. Miliary tuberculosis in a 3-year-old boy. Axial CT image (lung window) shows numerous small uniform nodules in both lungs without zonal predominance. Note the mediastinal and hilar lymphadenopathies (arrowheads).

of ill-defined nodules and the presence of cystic lesions (Fig 4) (39). Typically, miliary tuberculosis is characterized by numerous millimetric nodules in both lungs, with uniform distribution or lower zone predominance (Fig 5) (40). In addition, although the distinction is mostly based on the clinical picture, granulomatous and lymphocytic interstitial lung disease may also be included in the differential diagnosis. Because of similar systemic manifestations, such as lymphadenopathies, hepatosplenomegaly, and lung involvement, differentiation of sarcoidosis from common variable immunodeficiency–related granulomatous disease may be difficult at initial presentation (41). However, CT findings in granulomatous and lymphocytic interstitial lung disease such as bronchiectasis due to recurrent infections, nodules with lower zone dominance, and the halo sign are helpful in the differential diagnosis (42).

Another common finding in children is ground-glass opacity (Fig 6), but it occurs in less than one-half of adult patients (37,38). Ground-glass opacities are presumably due to airway compression caused by the coalescence of multiple interstitial granulomatous and fibrotic lesions, or mosaic attenuation due to involvement of small airways by granulomas (36). Interlobular septal thickening and consolidations are defined as atypical parenchymal findings in sarcoidosis and are reported less frequently in children as well as adults (37,38). Parenchymal abnormalities may progress to fibrosis in up to 20% of adult patients, and typical imaging findings are linear opacities, bronchial distortion, and honeycombing (Fig 7) (43,44). However, in children, pulmonary fibrosis and end-stage complications consisting of pulmonary hypertension and mycetoma are rare (7,16,38). In addition, rare atypical findings such as masslike opacities, cavitation, and pleural effusion have never been reported in children, to our knowledge.

Although CT and radiography are the most commonly used imaging techniques for mediastinal and pulmonary sarcoidosis, lung MRI is emerging as a radiation-free alternative (Fig 8). As a result of newly developed techniques, MRI has been shown to be increasingly useful in evaluating solid lung lesions, infections and their complications, and congenital malformations in children (24,45). MRI is known to have high sensitivity and specificity in patients with mediastinal and hilar lymphadenopathies of tuberculosis and parenchymal findings (40). Gorkem et al (46) showed similar results in childhood sarcoidosis and no difference between thoracic MRI and CT in detecting mediastinal lymphadenopathies and most of the parenchymal abnormalities including nodules, ground-glass opacities, and interlobular septal thickening. However, nodules smaller than 3 mm, mild ground-glass opacities, and cysts may not be detected with MRI. In addition, MRI can support the diagnosis on the basis of the signal intensity characteristics of the mediastinal lymph nodes. The "dark lymph node sign" defined in sarcoid lymphadenopathies refers to the central low signal intensity that may be associated with nodal fibrosis (47). However, this sign has not been demonstrated in children (46).

Cardiac Sarcoidosis

Cardiac involvement in sarcoidosis is rare in adults and even rarer in children. Clinical manifestations of cardiac disease include cardiomyopathy, heart block, arrhythmias, and sudden death (48). A definitive diagnosis of cardiac sarcoidosis is made by the detection of noncaseating granulomas at histopathologic examination; however, endomyocardial biopsy is an invasive procedure with a low diagnostic yield due to the focal involvement pattern of the disease (49). Cardiac involvement may be associated with high mortality; therefore, electrocardiography and echocardiography should be considered mandatory in the routine diagnostic workup. In addition, noninvasive imaging modalities are important in adult cardiac sarcoidosis, providing both diagnostic and prognostic information. Cardiac MRI or FDG PET/CT is recommended in adult patients with extracardiac sarcoidosis when cardiac symptoms and/or findings at electrocardiography or echocardiography are present (50). Because of the lack of pediatric recommendations, there are no data on the use of cardiac imaging in pediatric sarcoidosis. However, these imaging modalities may be useful for the diagnosis of clinically silent cardiac involvement and isolated cardiac sarcoidosis in children as well as in adults. Cardiac MRI has high sensitivity

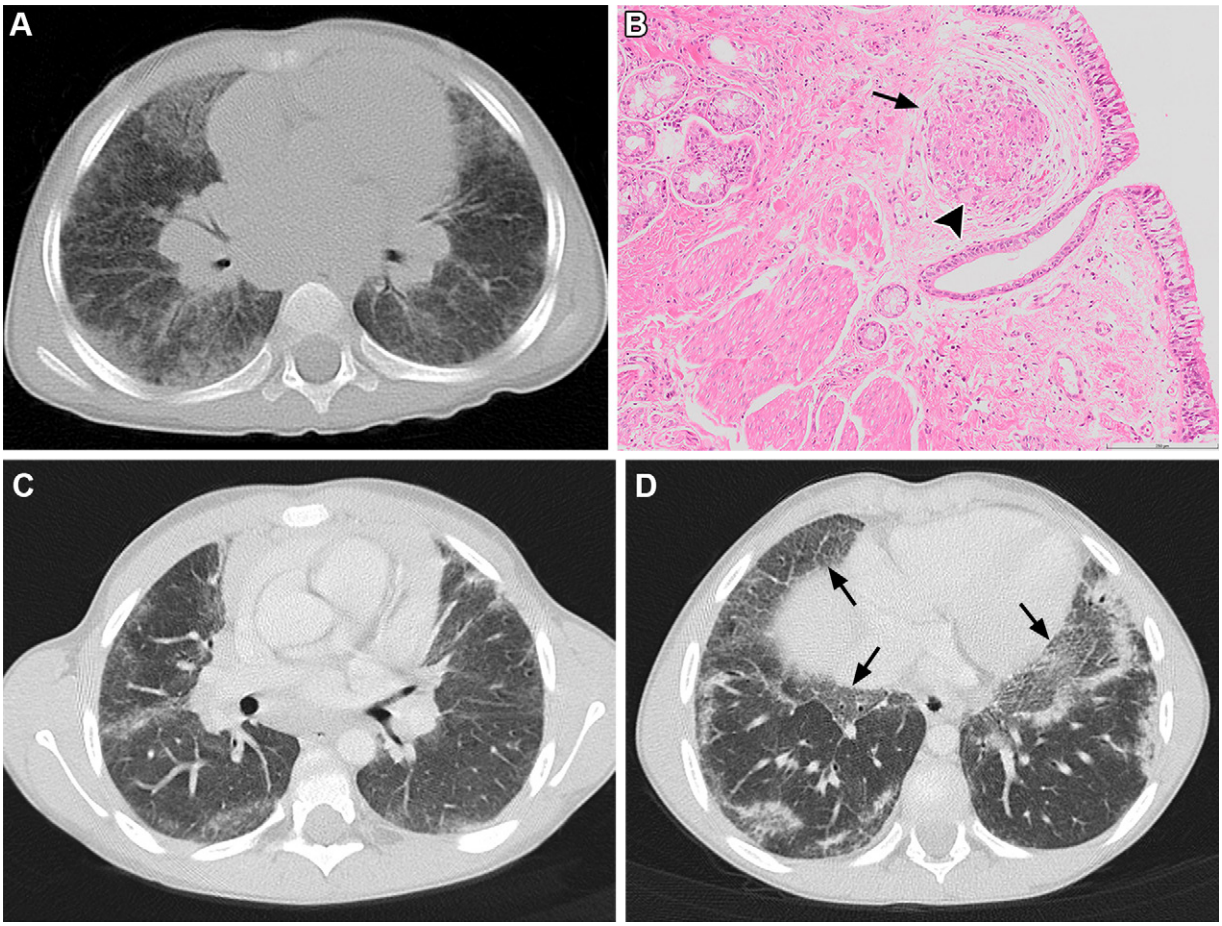

Figure 6. Pulmonary sarcoidosis in a 2-year-old boy with cough and dyspnea. At physical examination, oxygen saturation was low. **(A)** Axial CT image shows ground-glass opacities and nodular or granular opacities representing perilymphatic micronodules in both lungs. Note the symmetric hilar lymphadenopathies. **(B)** Photomicrograph of a transbronchial biopsy specimen shows small nonnecrotizing well-formed granulomas (arrow) beneath the respiratory epithelium. Granulomas were noncaseating and contained multinucleated giant cells (arrowhead) and epithelioid histiocytes surrounded by lymphocytes. Special histochemical stains on biopsy specimens with periodic acid-Schiff and Gomori methenamine silver stain (not shown) were negative for fungi, and Ziehl-Neelsen staining was negative for mycobacteria (not shown). The pathologic findings of granulomatous inflammation were considered to be consistent with a diagnosis of sarcoidosis. (Hematoxylin-eosin stain; original magnification, ×40.) **(C, D)** Axial CT images obtained 3 years after diagnosis show reticular opacities and ground-glass opacities. There is a "crazy-paving" pattern in both lower zones (arrows in **D**) and fibrosis with lower lung predominance, both of which are unusual in pulmonary sarcoidosis.

in diagnosis and high negative predictive value in ruling out cardiac involvement (51). At cardiac MRI, there is no pathognomonic imaging pattern for sarcoidosis, but midmyocardial and epicardial multifocal late gadolinium enhancement is often detected in the basal segments of the septum and lateral wall (52).

Abdominal Sarcoidosis

The abdomen is the most common extrapulmonary involvement site of sarcoidosis in children (53). The liver, spleen, and intra-abdominal lymph nodes are commonly involved; however, patients with abdominal disease are usually asymptomatic. Autopsy studies have demonstrated histologically evident hepatic and splenic involvement in more than one-half of patients (54). The most frequent abdominal findings in children at presentation are hepatomegaly, splenomegaly, and abdominal lymph node enlargement (53).

Hepatic and splenic sarcoidosis usually manifest as hepatosplenomegaly but may also manifest as multiple granulomatous nodules in the parenchyma (Fig 9) (53). Coalescence of noncaseous granulomas may appear as numerous small nodules at imaging (Fig 10). Children with suspected abdominal sarcoidosis are usually evaluated with US, which may show small multiple hypoechoic nodules in the liver and spleen. The differential diagnosis of these nodules includes metastases, lymphoma, and tuberculosis. In fact, CT is more sensitive than US in depicting small sarcoid nodules; however, ionizing radiation limits its use. MRI is presumably as sensitive as CT in showing hepatic and splenic nodular involvement. In addition, the signal intensity characteristics of sarcoid nodules at MRI, typically hypointense on images from all sequences, may help them to be distinguished from metastases and infections (55). However, sarcoid nodules may appear hyperintense on T2-weighted MR images in the presence of

Figure 7. Stage 4 pulmonary sarcoidosis in a 13-year-old adolescent girl. **(A, B)** Axial CT images show bronchiectasis (arrow in **A**), reticular and ground-glass opacities, and volume loss in the right upper lobe consistent with pulmonary fibrosis. Fibrotic changes can also be seen in the lower lobes (arrows in **B**). The patient underwent wedge biopsy of the lung and excisional biopsy of the hilar lymph nodes. Histopathologic examination of the biopsy specimens revealed nonnecrotizing granulomatous inflammation without any microorganisms. **(C)** Photomicrograph of lung biopsy specimen shows granulomas (arrow), which are composed of epithelioid and foamy macrophages bounded by lymphocytes and plasma cells. (Hematoxylin-eosin stain; original magnification, ×200.) **(D)** Photomicrograph of lymph node biopsy specimen shows granulomatous lymphadenitis and multinucleated giant cells, some of which have Schaumann bodies (arrow). (Hematoxylin-eosin stain; original magnification, ×400.)

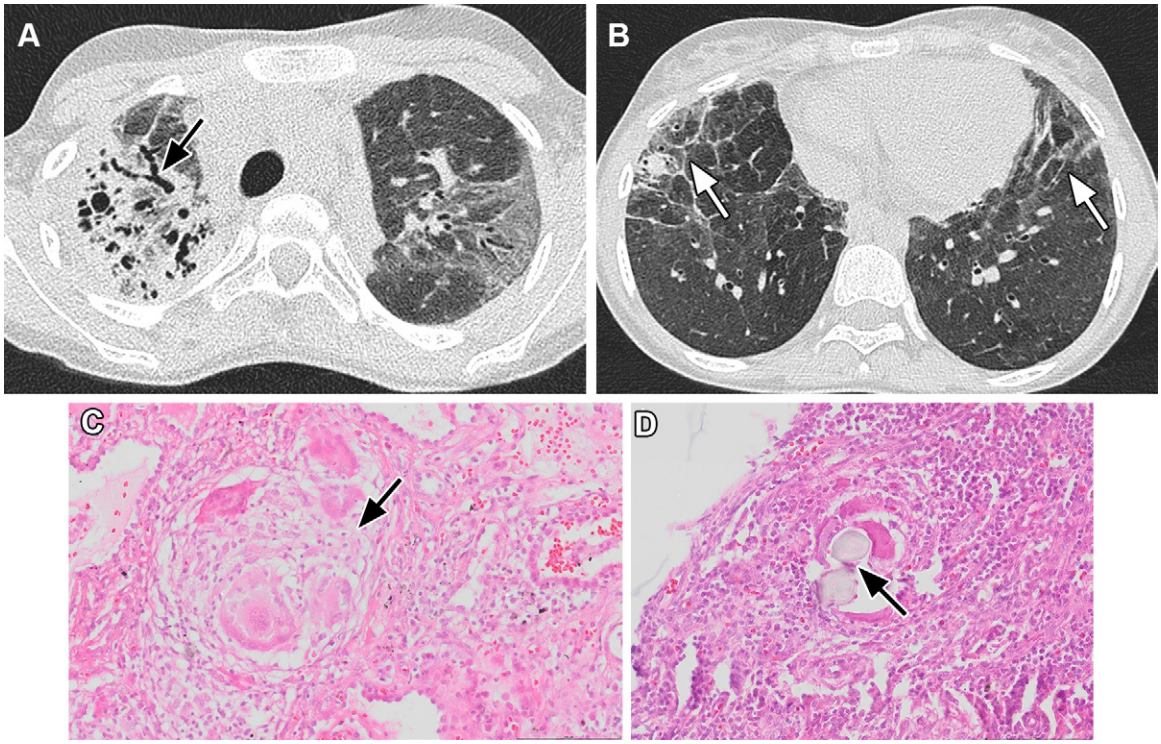

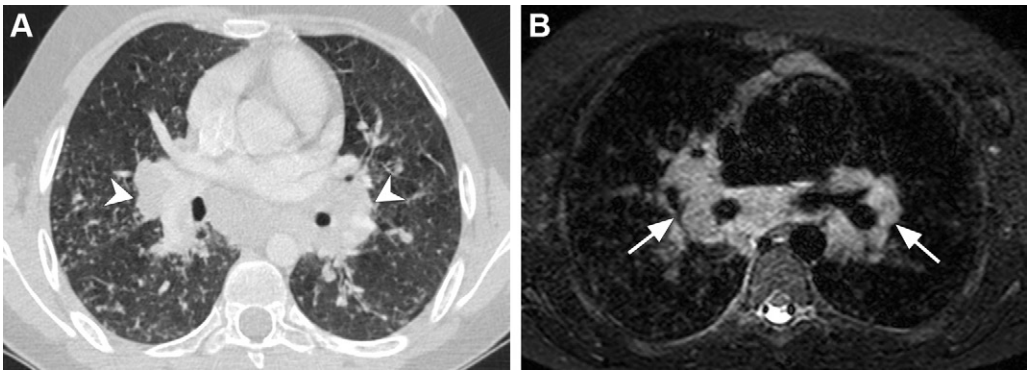

Figure 8. Pulmonary sarcoidosis in a 14-year-old adolescent boy. **(A)** Axial chest CT image (lung window) shows parenchymal micronodules and hilar lymphadenopathies (arrowheads). The patient's respiratory symptoms regressed with corticosteroid treatment, and follow-up MRI was performed. **(B)** Axial T2-weighted MR image shows bilateral symmetric hilar and mediastinal lymphadenopathies (arrows).

active inflammation and may show restricted diffusion at diffusion-weighted imaging (56). Biliary system involvement including subacute or chronic cholecystitis, cholestasis due to involvement of the hepatic ducts, and extrinsic compression of the biliary ducts by enlarged lymph nodes has been reported in adults (55) but not, to our knowledge, in children.

Gastrointestinal (GI) involvement infrequently occurs in children, with only a few cases being reported (53). The stomach is the most commonly involved organ in GI sarcoidosis, followed by the duodenum and esophagus (57). Diagnosis is usually made with histopathologic examination by means of endoscopic biopsy, and fluoroscopic studies can be complementary to examine luminal narrowing or obstruction due to intestinal wall involvement (58). The principal differential diagnosis in GI sarcoidosis is Crohn disease; unlike in sarcoidosis, GI involvement in Crohn disease is predominant.

Renal sarcoidosis commonly manifests as acute kidney failure in children (59). Renal disease is often related to hypercalcemia and hypercalciuria and can manifest as nephrocalcinosis and nephrolithiasis (59,60). Light microscopy may reveal granulomatous involvement in the kidneys and tubulointerstitial nephritis; however, disease that manifests radiologically occurs infrequently (59,60). Nephromegaly and heterogeneous enhancement can be seen at CT and MRI, whereas masslike

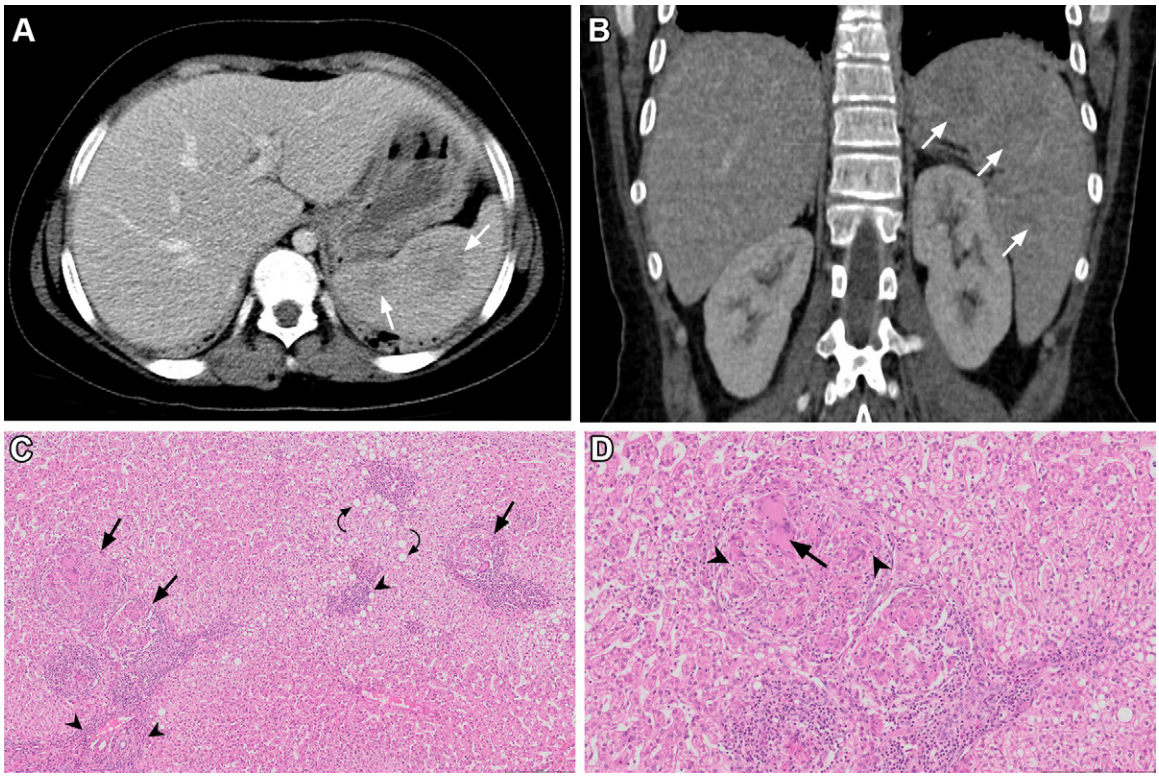

Figure 9. Abdominal sarcoidosis in an 11-year-old girl with fever, weight loss, and fatigue. Hepatosplenomegaly was detected at physical examination, and blood tests revealed elevated liver enzyme levels. **(A, B)** Axial **(A)** and coronal **(B)** reformatted contrast-enhanced abdominal CT images show splenomegaly and ill-defined hypoattenuating lesions in the spleen (arrows). No focal lesion is seen in the liver parenchyma. **(C)** Photomicrograph of the liver biopsy specimen revealed micro- and macrovesicular steatosis (curved arrows) with portal mononuclear inflammation (arrowheads) and multiple granulomas (straight arrows) adjacent to portal areas. (Hematoxylin-eosin stain; original magnification, ×40.) **(D)** Photomicrograph of stained biopsy specimen shows granulomas that did not have necrosis but rather consisted of epithelioid histiocytes, giant cells (arrow), and lymphocytes (arrowheads). (Hematoxylin-eosin stain; original magnification, ×200.)

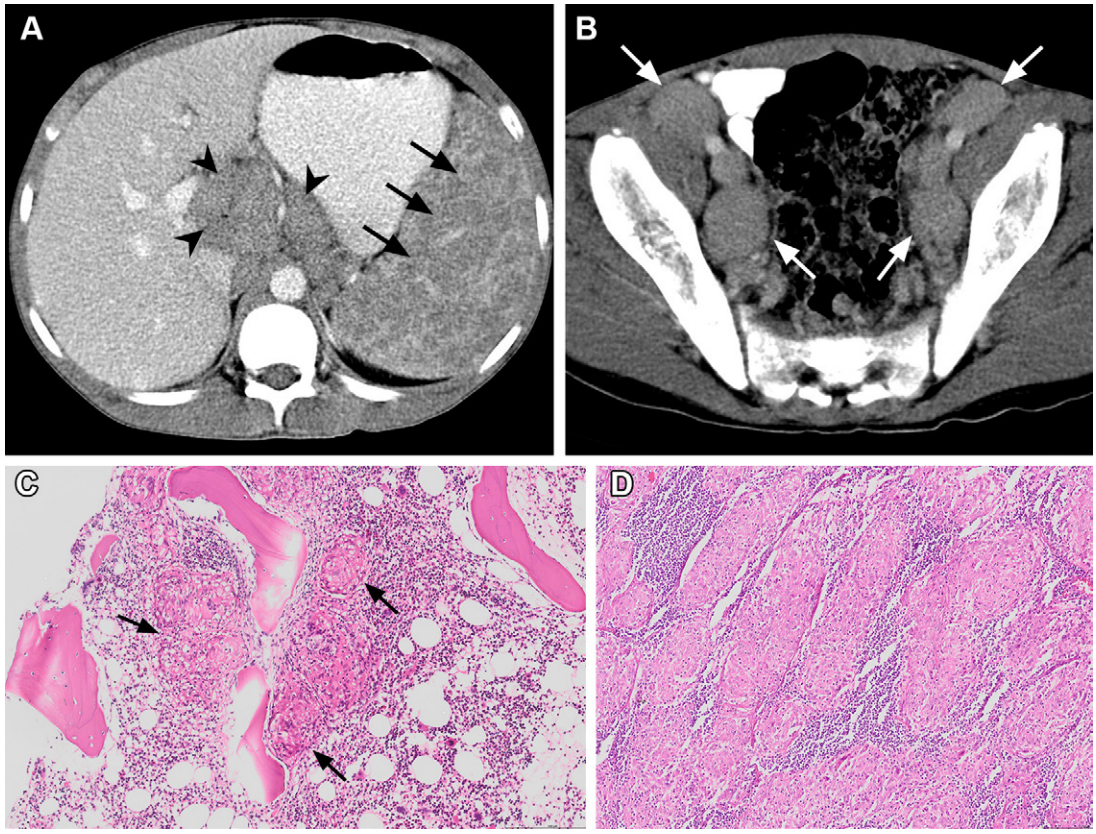

Figure 10. Abdominal sarcoidosis in a 16-year-old adolescent boy with fever and weight loss. Hepatosplenomegaly and cervical and inguinal lymphadenopathies were detected at physical examination. **(A)** Axial contrast-enhanced CT image shows splenomegaly and numerous small poorly defined hypoattenuating splenic lesions (arrows) and upper abdominal lymphadenopathies (arrowheads). **(B)** Axial CT image of the pelvis shows bilateral parailiac lymphadenopathies (arrows). **(C)** Photomicrograph of bone marrow biopsy specimen shows uniform multiple nonnecrotizing granulomas (arrows). (Hematoxylin-eosin stain; original magnification, ×200.) **(D)** Photomicrograph of the left jugulodigastric lymph node biopsy specimen shows granulomatous lymphadenitis, with granulomas obscuring the normal lymph node structure. (Hematoxylin-eosin stain; original magnification, ×400.)

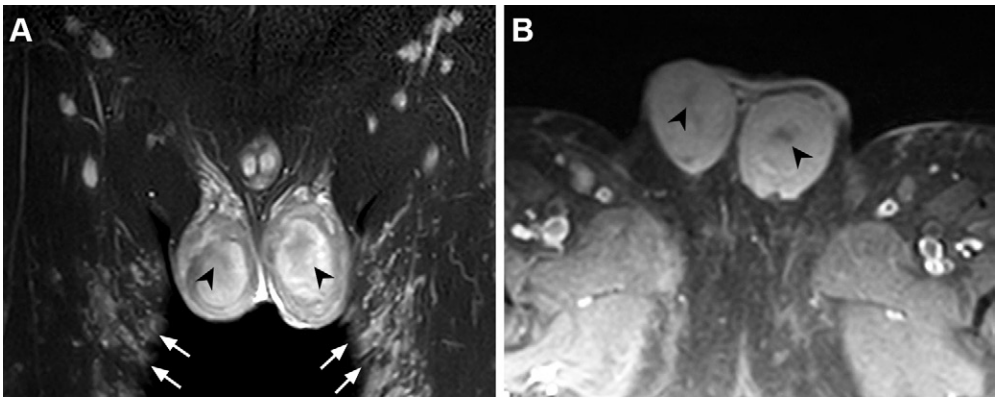

Figure 11. Testicular involvement in a 13-year-old adolescent boy. **(A)** Coronal fat-saturated T2-weighted MR image shows bilateral testicular enlargement and focal ill-defined hypointense lesions (arrowheads) in the parenchyma. Multiple small skin and subcutaneous lesions can be seen (arrows). **(B)** Postcontrast T1-weighted MR image shows heterogeneous enhancement of the testes with focal hypointense areas (arrowheads).

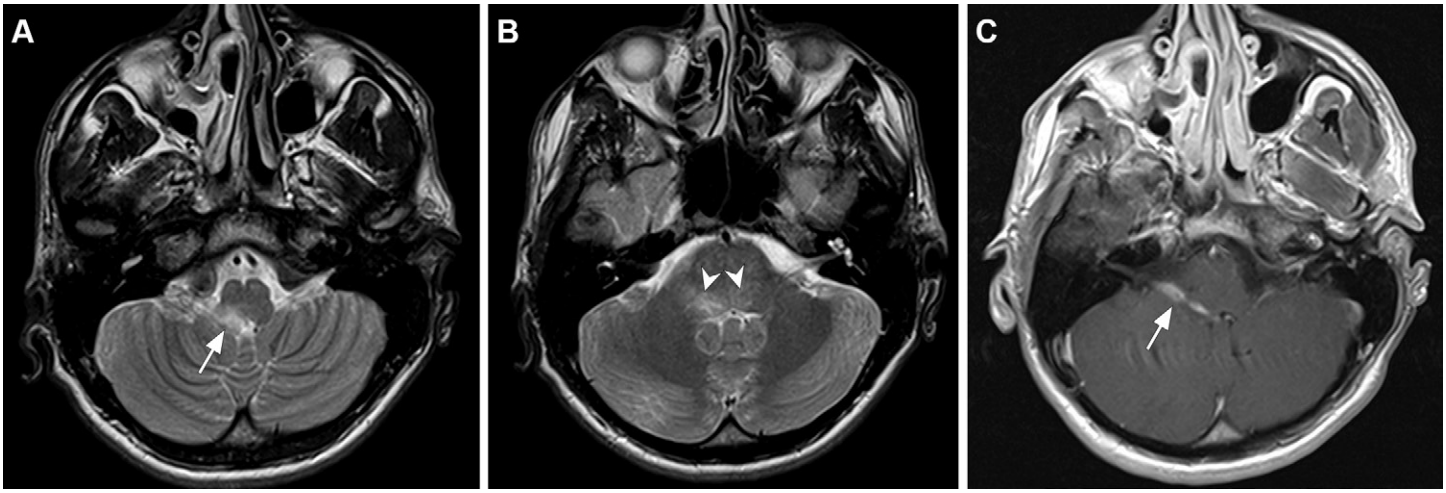

Figure 12. Neurosarcoidosis in an 18-year-old man. **(A, B)** Axial T2-weighted MR images show hyperintense lesions in the dorsal medulla oblongata (arrow in **A**) and pontin tegmentum (arrowheads in **B**). **(C)** Axial postcontrast T1-weighted MR image shows contrast enhancement of right cranial nerves VII and VIII (arrow).

hypovascular lesions mimicking tumors, lymphoma, or focal pyelonephritis are rarely seen in the renal parenchyma (61,62).

Testicular involvement in sarcoidosis is also reported in children, and the best imaging modality is US (63). Testicular disease often manifests with painless scrotal swelling, as in testicular tumors. The most common findings are unilateral or bilateral testicular enlargement and multifocal lesions (Fig 11). In rare cases, solitary lesions have also been reported (63). Hypointensity on T2-weighted MR images of solitary sarcoid lesions may help to differentiate them from tumors (55). However, histopathologic assessment is usually required because of the rarity of testicular sarcoidosis and its possible association with testicular cancer (64).

Neurosarcoidosis

Neurosarcoidosis is a rare manifestation of sarcoidosis in the pediatric age group, and most patients with central nervous system (CNS) involvement have systemic disease. Although isolated neurosarcoidosis is less common than systemic disease, a 2022 study (65) showed that isolated disease is more common in children than in adults. Patients with neurosarcoidosis can present with a variety of clinical findings, including seizures, cranial nerve palsies, hypothalamic dysfunctions, and spinal cord disorders (66). Although postpubertal patients are more likely to present with cranial nerve palsies as adults, prepubertal patients most commonly present with seizures (67).

The diagnosis is usually made according to cerebrospinal fluid (CSF) abnormalities, MRI findings consistent with neurosarcoidosis, and histopathologic examination of extraneural involvement (68). Imaging is essential to making the diagnosis, especially in patients with isolated CNS involvement for whom biopsy is not feasible. Sarcoid granulomas can affect any part of the nervous system, and imaging findings are mostly nonspecific. Therefore, the differential diagnosis encompasses a broad spectrum of CNS diseases. Examination of the CSF may reveal mononuclear pleocytosis, low glucose levels, elevated protein levels, and oligoclonal bands, which, although not specific for sarcoidosis, may provide evidence of active inflammation (68). The most common imaging findings in pediatric patients with neurosarcoidosis are leptomeningeal and cranial nerve enhancement, hypothalamic-pituitary involvement, and parenchymal disease manifesting as multiple subcortical and periventricular white matter lesions (65).

Cranial nerve involvement is a common manifestation of neurosarcoidosis in both children and adults (Fig 12). Although facial nerve palsy is the most common clinical finding in adults, the optic nerve is the most frequently affected cranial nerve in children, both radiologically and clinically

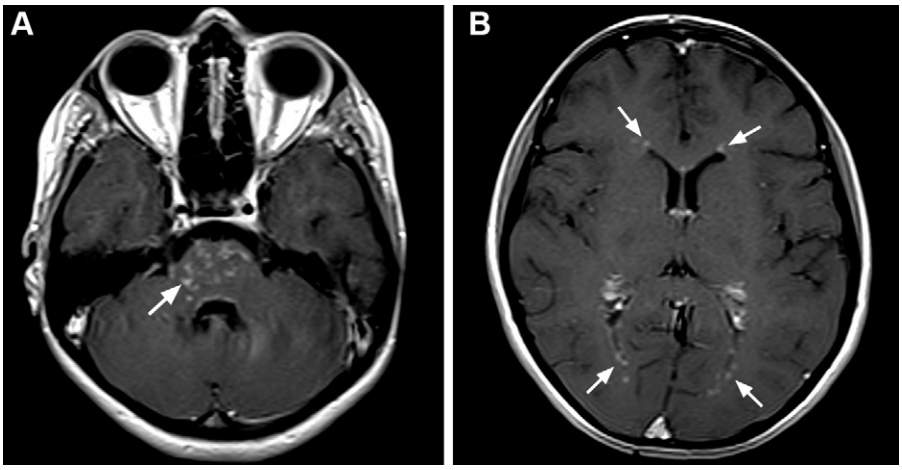

Figure 13. Neurosarcoidosis in a 16-year-old adolescent girl. Axial postcontrast T1-weighted MR images show multiple punctate areas of contrast enhancement suggesting perivascular involvement in the pons and the bilateral periventricular regions (arrows).

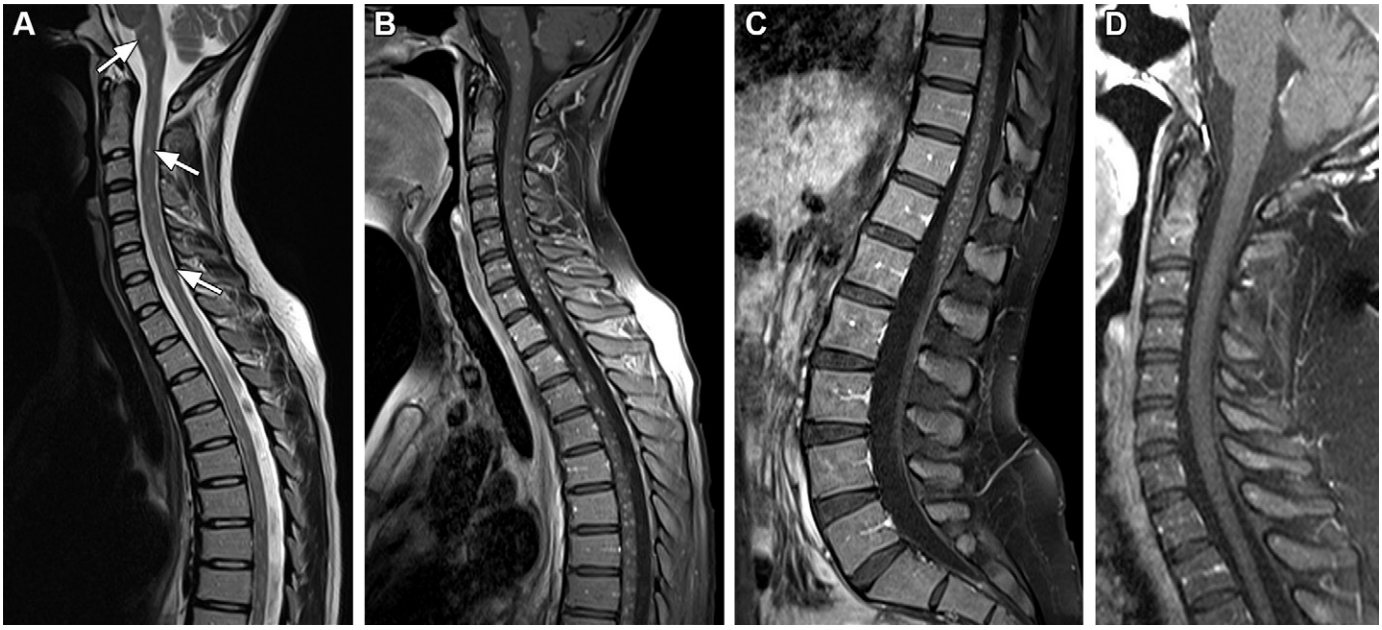

Figure 14. Neurosarcoidosis in a 17-year-old adolescent girl. **(A)** Sagittal T2-weighted MR image shows multiple subtle hyperintense cord lesions (arrows). **(B, C)** Sagittal postcontrast T1-weighted MR images show intramedullary holocord micronodular contrast enhancement. **(D)** Sagittal postcontrast T1-weighted MR image acquired after corticosteroid therapy shows no contrast-enhancing lesion in the cervical spinal cord.

(65,69). Cranial nerve involvement can be identified with contrast enhancement and enlargement of the affected cranial nerve. A cranial nerve deficit can be isolated or mostly concomitant with leptomeningeal involvement. Leptomeningeal involvement usually appears at MRI as diffuse or nodular thickening and contrast enhancement of the leptomeninges with a basilar predilection. The differential diagnosis for this basilar involvement pattern includes tuberculosis and lymphoma, and the imaging features of those are mostly indistinguishable. Hydrocephalus is another reported finding in children, possibly due to impaired CSF resorption or adhesions resulting from leptomeningeal involvement. Dural involvement is an unusual finding in children and may appear as a hypointense masslike lesion on T2-weighted MR images (70).

The involvement of the pituitary gland and hypothalamus, manifesting as diabetes insipidus and hypopituitarism, is also a well-known clinical picture of neurosarcoidosis in both children and adults (65,71). At MRI, thickening and enhancement of the infundibulum are common imaging features and mimic Langerhans cell histiocytosis. Parenchymal disease manifests as multiple small T2-hyperintense lesions, often with contrast enhancement, in periventricular white matter, the cerebellum, and brainstem (Fig 13). Enhancing mass lesions are rare but also can be seen in children. Small periventricular or parenchymal mass lesions may be indistinguishable from those seen in patients with multiple sclerosis, metastasis, or primary brain tumors. Although hypointensity on T2-weighted MR images has been described in masslike sarcoid brain lesions, this finding is not specific, because it can also be seen in cellular tumors, such as lymphoma (70).

Spinal neurosarcoidosis can manifest with intramedullary, intradural extramedullary, and extradural lesions at MRI. Spinal involvement has various imaging patterns, including fusiform spinal cord involvement, diffuse or focal leptomeningeal disease, or multiple punctate spinal cord lesions (Fig 14) (70). Spinal cord lesions usually occur

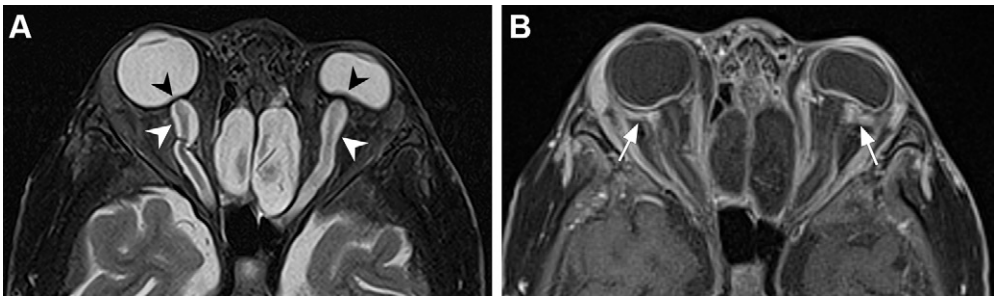

Figure 15. Systemic sarcoidosis in a 13-year-old adolescent boy. **(A)** Axial T2-weighted MR image shows scleral reverse cupping (black arrowheads) and left globe distortion. Note the enlargement of the perioptic CSF space (white arrowheads). **(B)** Axial postcontrast T1-weighted MR image shows contrast enhancement in the wall of the globe and postscleral fat tissue (arrows).

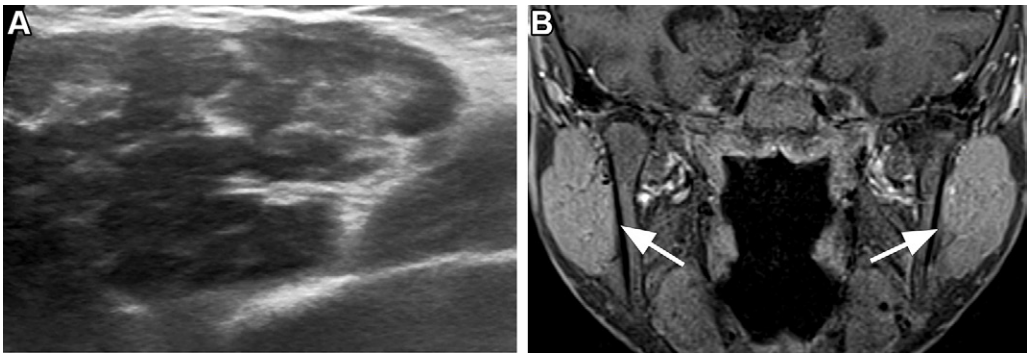

Figure 16. Bilateral parotid involvement in a 12-year-old boy with sarcoidosis. **(A)** US image shows right parotid gland enlargement and diffuse parenchymal heterogeneous hypoechogenicity. **(B)** Coronal postcontrast T1-weighted MR image shows bilateral parotid gland enlargement (arrows) without a focal lesion.

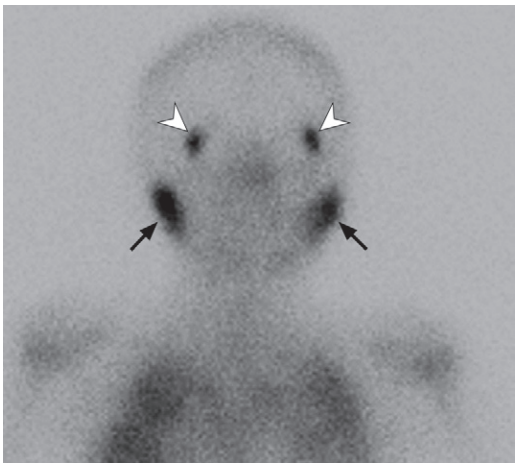

Figure 17. Lacrimal gland and parotid involvement in a 13-year-old adolescent girl. ^{67}Ga scintigram shows the "panda sign," increased uptake of radiotracer in the lacrimal (arrowheads) and parotid glands (arrows), with physiologic accumulation in the nasopharynx.

in the cervicothoracic part, are typically hyperintense on T2-weighted MR images, and often show contrast enhancement (72). Longitudinal extensive myelitis with or without leptomeningeal enhancement is considered the classic imaging pattern of spinal sarcoidosis (72). Crescent-shaped dorsal subpial enhancement accompanied by central canal enhancement (ie, the "trident sign") (73) should also be considered as a clue to spinal sarcoidosis. However, to our knowledge, this sign has not been demonstrated in children.

Head and Neck Sarcoidosis

A broad spectrum of head and neck manifestations of sarcoidosis may exist. Any structure in the head and neck may be involved, including the orbital structures, cervical lymph nodes, salivary and thyroid glands, pharynx, and larynx.

Orbital disease may occur in 29%–74% of pediatric patients with sarcoidosis (Fig 15) (1). Although any orbital structure can be involved, ocular involvement most commonly manifests as uveitis in children. Eye pain, redness, and blurry vision are common symptoms, and diagnosis is mostly made by clinical examination. The lacrimal gland is a common extraocular involvement site in the orbit, and patients may present with upper eyelid swelling and dry eyes. CT and MRI reveal diffuse enlargement and enhancement of the lacrimal gland, with or without adjacent fat stranding. Extraocular muscles and retrobulbar fat tissue may be involved in adults, but, to our knowledge, this has not been reported in children.

Parotid involvement can be seen in 30% of pediatric patients with sarcoidosis, with mostly parotid gland swelling (Fig 16) (7). Facial nerve palsy may be seen with parotid involvement. US may show enlargement and heterogeneous hypoechogenicity in the parotid parenchyma. The affected gland often shows increased signal intensity on T2-weighted MR images, with homogeneous enhancement at MRI. ^{67}Ga imaging may demonstrate abnormal uptake in bilateral parotid and lacrimal glands, with physiologic uptake in the nasopharyngeal mucosa (74). These findings are often cited as the "panda sign" (Fig 17). However, this classic radiologic sign is mostly of historical interest in the current era because ^{67}Ga imaging is often replaced with FDG PET/CT.

The larynx is rarely involved in children and adults with sarcoidosis. Laryngeal sarcoidosis has a predilection for supraglottic structures, including the epiglottis, aryepiglottic folds, and arytenoids. Patients with epiglottic involvement may present with a sore throat, hoarseness, and dysphagia (75). CT and MRI may show nonspecific findings including edema, contrast enhancement, and nodular thickening in affected structures.

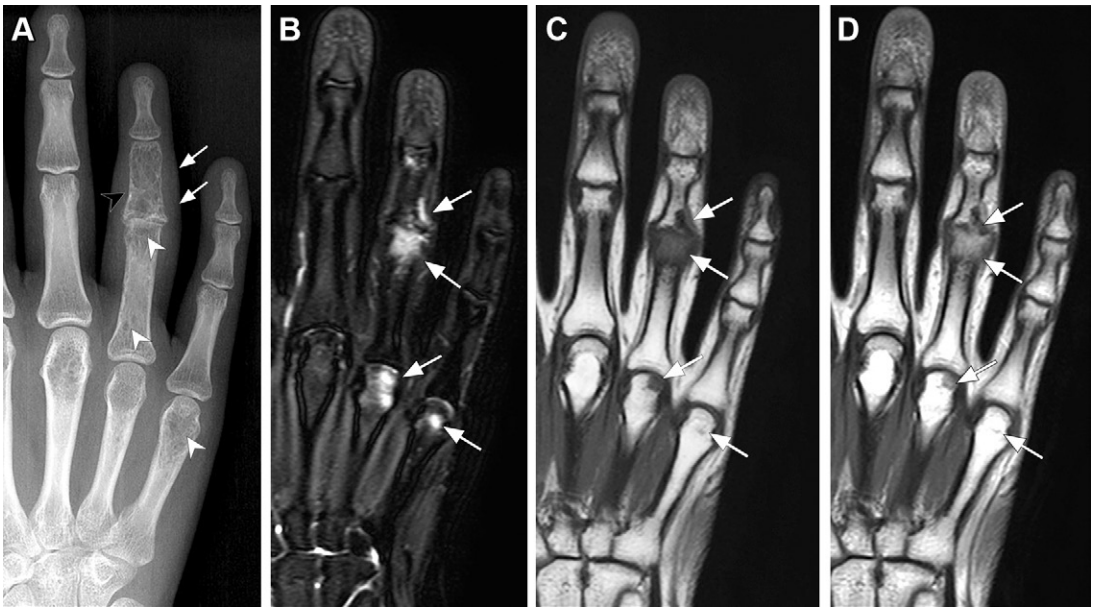

Figure 18. Small bone sarcoidosis in a 17-year-old adolescent girl who presented with swelling of the left fourth finger. **(A)** Radiograph of the left hand shows soft-tissue swelling (arrows) and a lacelike lytic pattern (black arrowhead) in the middle phalanx of the fourth finger, with multiple well-defined lytic lesions in the phalanges and metacarpal bones (arrowheads). **(B–D)** MR images obtained after corticosteroid therapy show that the soft-tissue swelling and bone lesions have regressed. Coronal fat-saturated T2-weighted MR image **(B)** shows residual intramedullary lesions in the phalanges and metacarpal bones (arrows). Coronal precontrast **(C)** and postcontrast **(D)** T1-weighted MR images show contrast enhancement in the lesions (arrows).

Musculoskeletal Sarcoidosis

Sarcoidosis granulomas can involve bones, joints, and muscles. Although arthritis is the most common form of musculoskeletal sarcoidosis in children, radiologically evident involvement is relatively rare. Chronic nonerosive polyarthritis affecting the appendicular skeleton, particularly the knees, ankles, wrists, and proximal interphalangeal joints, is a common feature of sarcoid joint disease (76). Juvenile idiopathic arthritis is the main consideration in the differential diagnosis of sarcoid joint disease. Monoarthritis is unusual in patients with sarcoidosis.

Bone lesions in patients with sarcoidosis most frequently occur in the phalanges of the hands and feet. The characteristic radiographic features of small bone sarcoidosis are lacelike lytic lesions with thickened trabeculae (77). MRI can demonstrate radiographically occult bone marrow lesions and extension of lesions beyond the cortex (Fig 18). Long bones and the axial skeleton are relatively uncommon involvement sites; however, these are probably underestimated due to asymptomatic involvement (78). Cortical destruction is not a common feature of long bone lesions; thus, they are usually occult on radiographs. Diagnosis of these lesions, even if they are visible on radiographs, is still challenging because of various imaging patterns ranging from well-defined lesions to permeative patterns. Sarcoid bone lesions lack specific signal intensity characteristics, appear hypointense at T1-weighted MRI and hyperintense at T2-weighted MRI, and show variable enhancement on postcontrast MR images. Hematologic malignancies, metastasis, and chronic disseminated infections (eg, tuberculosis) should be considered in the differential diagnosis.

Sarcoid myopathy may manifest as acute or chronic diffuse myositis or as a nodular form usually associated with palpable lesions (78). Although isolated muscle involvement is rare, it may be an initial manifestation of sarcoidosis in children (79). Granulomatous myositis in sarcoidosis may resemble other generalized myopathies clinically and radiologically (eg, polymyositis). The differentiation between them is usually made by tissue biopsy of the affected muscle. On the other hand, nodular sarcoid myopathy manifests as focal soft-tissue masses, often in the lower extremities, causing a more substantial diagnostic challenge. Rhabdomyosarcoma, the most common malignant soft-tissue tumor in children, is the principal consideration in the differential diagnosis. However, on T2-weighted MR images, a hypointense starlike shape in the center and a hyperintense rim in the periphery, which often is referred to as the "dark star" appearance, may be useful in differentiating sarcoid nodules from soft-tissue tumors (78).

Subcutaneous granulomatous infiltration can be present as discrete or indistinct nonspecific soft-tissue lesions. These lesions may be hypoechoic at US and may show nonspecific signal intensity at MRI, with a variable contrast enhancement pattern (Fig 19) (77). Differentiation between subcutaneous sarcoid nodules and benign or malignant mesenchymal masses can be difficult, and histopathologic examination is usually required.

Conclusion

Pediatric sarcoidosis is a rare but important disease that can result in substantial morbidity and is usually distinctly different from adult sarcoidosis. The diagnosis of childhood sarcoidosis is often delayed considerably because of the wide

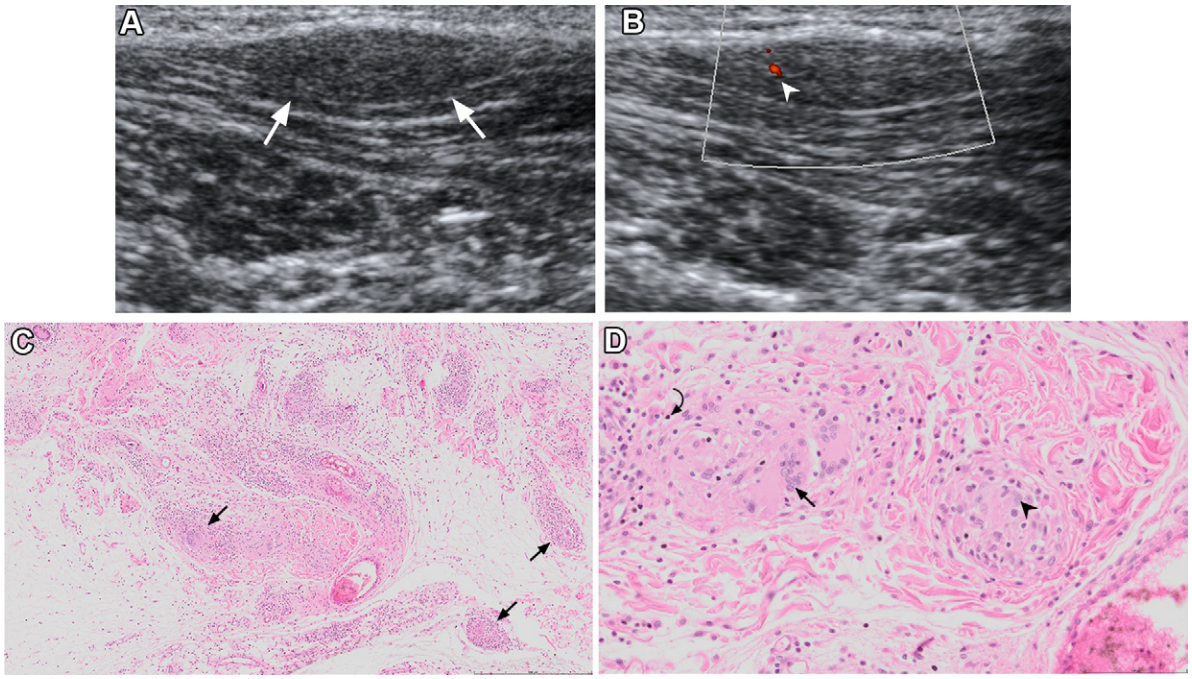

Figure 19. Pulmonary sarcoidosis in an 11-year-old boy who presented with a palpable nodule on the left forearm. **(A, B)** US images show a well-defined hypoechoic solid mass (arrows in **A**) with minimal vascularization (arrowhead in **B**) in the subcutaneous fat tissue at Doppler US. **(C)** Photomicrograph of an excisional biopsy specimen from the subcutaneous nodule shows uniform-sized granulomas (arrows) in subcutaneous mature fat tissue. (Hematoxylin-eosin stain; original magnification, ×40.) **(D)** Photomicrograph of the biopsy specimen shows granulomas composed of epithelioid histiocytes (arrowhead) and multinuclear giant cells (straight arrow) surrounded by lymphocytes (curved arrow). (Hematoxylin-eosin stain; original magnification, ×400.)

spectrum of clinical manifestations, depending on patient age. Imaging is essential in the diagnosis of pediatric sarcoidosis, in assessing the extent of the disease, and in monitoring response to treatment. Therefore, radiologists' familiarity with the patterns of systemic involvement and imaging findings is critical for timely diagnosis and management of the disease.

Author affiliations.—From the Departments of Radiology (G.O., H.N.O., R.G., B.O., M.H.) and Pathology (D.O.), Hacettepe University School of Medicine, Hacettepe M, Gevher Nesibe C, 06230 Altındag/Ankara, Turkey. Presented as an education exhibit at the 2022 RSNA Annual Meeting. Received April 29, 2023; revision requested June 9 and received June 18; accepted July 12. **Address correspondence to** G.O. (email: *gozdetufan@gmail.com*).

Disclosures of conflicts of interest.—All authors, the editor, and the reviewers have disclosed no relevant relationships.

References

1. Nathan N, Sileo C, Calender A, et al. Paediatric sarcoidosis. Paediatr Respir Rev 2019;29:53–59.
2. Arkema EV, Cozier YC. Sarcoidosis epidemiology: recent estimates of incidence, prevalence and risk factors. Curr Opin Pulm Med 2020;26(5):527–534.
3. Cone RB. A review of Boeck's sarcoid with analysis of 12 cases occurring in children. J Pediatr 1948;32(6):629–640.
4. Nathan N, Marcelo P, Houdouin V, et al. Lung sarcoidosis in children: update on disease expression and management. Thorax 2015;70(6):537–542.
5. Gedalia A, Khan TA, Shetty AK, Dimitriades VR, Espinoza LR. Childhood sarcoidosis: Louisiana experience. Clin Rheumatol 2016;35(7):1879–1884.
6. Hoffmann AL, Milman N, Byg KE. Childhood sarcoidosis in Denmark 1979-1994: incidence, clinical features and laboratory results at presentation in 48 children. Acta Paediatr 2004;93(1):30–36.
7. Nott K, Nott V, Lever E, et al. Pediatric sarcoidosis: retrospective analysis of biopsy-proven patients. J Rheumatol 2023;50(7):924–933.
8. Cimaz R, Ansell BM. Sarcoidosis in the pediatric age. Clin Exp Rheumatol 2002;20(2):231–237.
9. Fretzayas A, Moustaki M, Vougiouka O. The puzzling clinical spectrum and course of juvenile sarcoidosis. World J Pediatr 2011;7(2):103–110.
10. Kaufman KP, Becker ML. Distinguishing Blau syndrome from systemic sarcoidosis. Curr Allergy Asthma Rep 2021;21(2):10.
11. Rossides M, Grunewald J, Eklund A, et al. Familial aggregation and heritability of sarcoidosis: a Swedish nested case-control study. Eur Respir J 2018;52(2):1800385.
12. Nathan N, Montagne ME, Macchi O, et al. Exposure to inorganic particles in paediatric sarcoidosis: the PEDIASARC study. Thorax 2022;77(4):404–407.
13. Ma Y, Gal A, Koss MN. The pathology of pulmonary sarcoidosis: update. Semin Diagn Pathol 2007;24(3):150–161.
14. Grunewald J, Grutters JC, Arkema EV, Saketkoo LA, Moller DR, Müller-Quernheim J. Sarcoidosis. Nat Rev Dis Primers 2019;5(1):45 [Published correction appears in Nat Rev Dis Primers 2019;5(1):49.].
15. Baughman RP, Teirstein AS, Judson MA, et al; Case Control Etiologic Study of Sarcoidosis (ACCESS) research group. Clinical characteristics of patients in a case control study of sarcoidosis. Am J Respir Crit Care Med 2001;164(10 Pt 1):1885–1889.
16. Chauveau S, Jeny F, Montagne ME, et al. Child–adult transition in sarcoidosis: a series of 52 Patients. J Clin Med 2020;9(7):2097.
17. Shetty AK, Gedalia A. Childhood sarcoidosis: a rare but fascinating disorder. Pediatr Rheumatol Online J 2008;6(1):16.
18. Drent M, Crouser ED, Grunewald J. Challenges of sarcoidosis and its management. N Engl J Med 2021;385(11):1018–1032.
19. Fauroux B, Clément A. Paediatric sarcoidosis. Paediatr Respir Rev 2005;6(2):128–133.
20. Milman N, Svendsen CB, Hoffmann AL. Health-related quality of life in adult survivors of childhood sarcoidosis. Respir Med 2009;103(6):913–918.
21. Chiu B, Chan J, Das S, Alshamma Z, Sergi C. Pediatric sarcoidosis: a review with emphasis on early onset and high-Risk Sarcoidosis and Diagnostic Challenges. Diagnostics (Basel) 2019;9(4):160.
22. Kraaijvanger R, Janssen Bonás M, Vorselaars ADM, Veltkamp M. Biomarkers in the diagnosis and prognosis of sarcoidosis: current use and future prospects. Front Immunol 2020;11:1443.

23. Crouser ED, Maier LA, Wilson KC, et al. Diagnosis and detection of sarcoidosis. An official American Thoracic Society clinical practice guideline. Am J Respir Crit Care Med 2020;201(8):e26–e51.
24. Serai SD, Rapp JB, States LJ, Andronikou S, Ciet P, Lee EY. Pediatric lung MRI: currently available and emerging techniques. AJR Am J Roentgenol 2021;216(3):781–790.
25. Akaike G, Itani M, Shah H, et al. PET/CT in the diagnosis and workup of sarcoidosis: focus on atypical manifestations. RadioGraphics 2018;38(5):1536–1549.
26. Baculard A, Blanc N, Boulé M, et al. Pulmonary sarcoidosis in children: a follow-up study. Eur Respir J 2001;17(4):628–635.
27. Pattishall EN, Kendig EL Jr. Sarcoidosis in children. Pediatr Pulmonol 1996;22(3):195–203.
28. Copley SJ, Coren M, Nicholson AG, Rubens MB, Bush A, Hansell DM. Diagnostic accuracy of thin-section CT and chest radiography of pediatric interstitial lung disease. AJR Am J Roentgenol 2000;174(2):549–554.
29. Scadding JG. Prognosis of intrathoracic sarcoidosis in England. A review of 136 cases after five years' observation. BMJ 1961;2(5261):1165–1172.
30. Keesling CA, Frush DP, O'Hara SM, Fordham LA. Clinical and imaging manifestations of pediatric sarcoidosis. Acad Radiol 1998;5(2):122–132.
31. Milman N, Hoffmann AL. Childhood sarcoidosis: long-term follow-up. Eur Respir J 2008;31(3):592–598.
32. Biko DM, Lichtenberger JP 3rd, Rapp JB, Khwaja A, Huppmann AR, Chung EM. Mediastinal masses in children: radiologic-pathologic correlation. RadioGraphics 2021;41(4):1186–1207.
33. Nunes H, Uzunhan Y, Gille T, Lamberto C, Valeyre D, Brillet PY. Imaging of sarcoidosis of the airways and lung parenchyma and correlation with lung function. Eur Respir J 2012;40(3):750–765.
34. Ganeshan D, Menias CO, Lubner MG, Pickhardt PJ, Sandrasegaran K, Bhalla S. Sarcoidosis from head to toe: what the radiologist needs to know. RadioGraphics 2018;38(4):1180–1200.
35. Lee GM, Pope K, Meek L, Chung JH, Hobbs SB, Walker CM. Sarcoidosis: a diagnosis of exclusion. AJR Am J Roentgenol 2020;214(1):50–58.
36. Criado E, Sánchez M, Ramírez J, et al. Pulmonary sarcoidosis: typical and atypical manifestations at high-resolution CT with pathologic correlation. RadioGraphics 2010;30(6):1567–1586.
37. Vrielynck S, Mamou-Mani T, Emond S, Scheinmann P, Brunelle F, de Blic J. Diagnostic value of high-resolution CT in the evaluation of chronic infiltrative lung disease in children. AJR Am J Roentgenol 2008;191(3):914–920.
38. Sileo C, Epaud R, Mahloul M, et al. Sarcoidosis in children: HRCT findings and correlation with pulmonary function tests. Pediatr Pulmonol 2014;49(12):1223–1233.
39. Bano S, Chaudhary V, Narula MK, et al. Pulmonary Langerhans cell histiocytosis in children: a spectrum of radiologic findings. Eur J Radiol 2014;83(1):47–56.
40. Sodhi KS, Bhalla AS, Mahomed N, Laya BF. Imaging of thoracic tuberculosis in children: current and future directions. Pediatr Radiol 2017;47(10):1260–1268.
41. Maccora I, Marrani E, Ricci S, et al. Common variable immunodeficiency presenting as sarcoidosis in a 9-year-old child. Int J Rheum Dis 2020;23(3):448–453.
42. Verbsky JW, Routes JM. Sarcoidosis and common variable immunodeficiency: similarities and differences. Semin Respir Crit Care Med 2014;35(3):330–335.
43. Abehsera M, Valeyre D, Grenier P, Jaillet H, Battesti JP, Brauner MW. Sarcoidosis with pulmonary fibrosis: CT patterns and correlation with pulmonary function. AJR Am J Roentgenol 2000;174(6):1751–1757.
44. Patterson KC, Strek ME. Pulmonary fibrosis in sarcoidosis. Clinical features and outcomes. Ann Am Thorac Soc 2013;10(4):362–370.
45. Ozcan HN, Gormez A, Ozsurekci Y, et al. Magnetic resonance imaging of pulmonary infection in immunocompromised children: comparison with multidetector computed tomography. Pediatr Radiol 2017;47(2):146–153.
46. Gorkem SB, Köse S, Lee EY, Doğanay S, Coskun AS, Köse M. Thoracic MRI evaluation of sarcoidosis in children. Pediatr Pulmonol 2017;52(4):494–499.
47. Chung JH, Cox CW, Forssen AV, Biederer J, Puderbach M, Lynch DA. The dark lymph node sign on magnetic resonance imaging: a novel finding in patients with sarcoidosis. J Thorac Imaging 2014;29(2):125–129.
48. Duke C, Rosenthal E. Sudden death caused by cardiac sarcoidosis in childhood. J Cardiovasc Electrophysiol 2002;13(9):939–942.
49. Birnie DH, Nery PB, Ha AC, Beanlands RSB. Cardiac sarcoidosis. J Am Coll Cardiol 2016;68(4):411–421.
50. Tan JL, Tan BE, Cheung JW, Ortman M, Lee JZ. Update on cardiac sarcoidosis. Trends Cardiovasc Med 2022. 10.1016/j.tcm.2022.04.007. Published online April 30, 2022.
51. Kouranos V, Tzelepis GE, Rapti A, et al. Complementary role of CMR to conventional screening in the diagnosis and prognosis of cardiac sarcoidosis. JACC Cardiovasc Imaging 2017;10(12):1437–1447.
52. Jeudy J, Burke AP, White CS, Kramer GBG, Frazier AA. Cardiac sarcoidosis: the challenge of radiologic-pathologic correlation: from the radiologic pathology archives. RadioGraphics 2015;35(3):657–679.
53. Morel B, Sileo C, Epaud R, et al. Ultrasonography and computed tomographic manifestations of abdominal sarcoidosis in children. J Pediatr Gastroenterol Nutr 2016;63(2):195–199.
54. Koyama T, Ueda H, Togashi K, Umeoka S, Kataoka M, Nagai S. Radiologic manifestations of sarcoidosis in various organs. RadioGraphics 2004;24(1):87–104.
55. Gezer NS, Başara I, Altay C, et al. Abdominal sarcoidosis: cross-sectional imaging findings. Diagn Interv Radiol 2015;21(2):111–117.
56. Sekine T, Amano Y, Hidaka F, et al. Hepatosplenic and muscular sarcoidosis: characterization with MR imaging. Magn Reson Med Sci 2012;11(2):83–89.
57. Brito-Zerón P, Bari K, Baughman RP, Ramos-Casals M. Sarcoidosis involving the gastrointestinal tract: diagnostic and therapeutic management. Am J Gastroenterol 2019;114(8):1238–1247.
58. Noël JM, Katona IM, Piñeiro-Carrero VM. Sarcoidosis resulting in duodenal obstruction in an adolescent. J Pediatr Gastroenterol Nutr 1997;24(5):594–598.
59. Klaus R, Jansson AF, Griese M, Seeman T, Amann K, Lange-Sperandio B. Case Report: Pediatric renal sarcoidosis and prognostic factors in reviewed cases. Front Pediatr 2021;9:724728.
60. Coutant R, Leroy B, Niaudet P, et al. Renal granulomatous sarcoidosis in childhood: a report of 11 cases and a review of the literature. Eur J Pediatr 1999;158(2):154–159.
61. Herman TE, Shackelford GD, McAlister WH. Pseudotumoral sarcoid granulomatous nephritis in a child: case presentation with sonographic and CT findings. Pediatr Radiol 1997;27(9):752–754.
62. Warshauer DM, Lee JK. Imaging manifestations of abdominal sarcoidosis. AJR Am J Roentgenol 2004;182(1):15–28.
63. Evans SS, Fisher RG, Scott MA, Kennedy BG, Brock JW 3rd, Wilson GJ. Sarcoidosis presenting as bilateral testicular masses. Pediatrics 1997;100(3 Pt 1):392–394.
64. Dick J, Begent RH, Meyer T. Sarcoidosis and testicular cancer: a case series and literature review. Urol Oncol 2010;28(4):350–354.
65. Young M, Goldman-Yassen A, Anderson M, et al. Neurosarcoidosis in children: a systematic review and summary of cases, imaging and management. J Neuroimmunol 2022;371:577938.
66. Rao R, Dimitriades VR, Weimer M, Sandlin C. Neurosarcoidosis in pediatric patients: a case report and review of isolated and systemic neurosarcoidosis. Pediatr Neurol 2016;63:45–52.
67. Baumann RJ, Robertson WC Jr. Neurosarcoid presents differently in children than in adults. Pediatrics 2003;112(6 Pt 1):e480–e486.
68. Stern BJ, Royal W 3rd, Gelfand JM, et al. Definition and consensus diagnostic criteria for neurosarcoidosis: from the Neurosarcoidosis Consortium Consensus Group. JAMA Neurol 2018;75(12):1546–1553.
69. Bathla G, Freeman CW, Moritani T, et al. Retrospective, dual-centre review of imaging findings in neurosarcoidosis at presentation: prevalence and imaging sub-types. Clin Radiol 2020;75(10):796.e1–796.e9.
70. Smith JK, Matheus MG, Castillo M. Imaging manifestations of neurosarcoidosis. AJR Am J Roentgenol 2004;182(2):289–295.
71. Langrand C, Bihan H, Raverot G, et al. Hypothalamo-pituitary sarcoidosis: a multicenter study of 24 patients. QJM 2012;105(10):981–995.
72. Murphy OC, Salazar-Camelo A, Jimenez JA, et al. Clinical and MRI phenotypes of sarcoidosis-associated myelopathy. Neurol Neuroimmunol Neuroinflamm 2020;7(4):e722.
73. Zalewski NL, Krecke KN, Weinshenker BG, et al. Central canal enhancement and the trident sign in spinal cord sarcoidosis. Neurology 2016;87(7):743–744.
74. Chapman MN, Fujita A, Sung EK, et al. Sarcoidosis in the head and neck: an illustrative review of clinical presentations and imaging findings. AJR Am J Roentgenol 2017;208(1):66–75.
75. McHugh K, deSilva M, Kilham HA. Epiglottic enlargement secondary to laryngeal sarcoidosis. Pediatr Radiol 1993;23(1):71.
76. Navallas M, Inarejos Clemente EJ, Iglesias E, Rebollo-Polo M, Zaki FM, Navarro OM. Autoinflammatory diseases in childhood, part 1: monogenic syndromes. Pediatr Radiol 2020;50(3):415–430.
77. Moore SL, Teirstein AE. Musculoskeletal sarcoidosis: spectrum of appearances at MR imaging. RadioGraphics 2003;23(6):1389–1399.
78. Brandão Guimarães J, Nico MA, Omond AG, et al. Radiologic manifestations of musculoskeletal sarcoidosis. Curr Rheumatol Rep 2019;21(3):7.
79. Orandi AB, Eutsler E, Ferguson C, White AJ, Kitcharoensakkul M. Sarcoidosis presenting as granulomatous myositis in a 16-year-old adolescent. Pediatr Rheumatol Online J 2016;14(1):59.